NASA/TM—2001-211138 IECEC2001–AT–10

International Space Station Bus Regulation With NASA Glenn Research Center Flywheel Energy Storage System Development Unit

Peter E. Kascak
Ohio Aerospace Institute, Brook Park, Ohio

Barbara H. Kenny
Glenn Research Center, Cleveland, Ohio

Timothy P. Dever
QSS Group, Inc., Brook Park, Ohio

Walter Santiago
Glenn Research Center, Cleveland, Ohio

Ralph H. Jansen
Ohio Aerospace Institute, Brook Park, Ohio

Prepared for the
36th Intersociety Energy Conversion Engineering Conference
cosponsored by the ASME, IEEE, AIChE, ANS, SAE, and AIAA
Savannah, Georgia, July 29–August 2, 2001

National Aeronautics and
Space Administration

Glenn Research Center

September 2001

Available from

NASA Center for Aerospace Information
7121 Standard Drive
Hanover, MD 21076

National Technical Information Service
5285 Port Royal Road
Springfield, VA 22100

Available electronically at http://gltrs.grc.nasa.gov/GLTRS

INTERNATIONAL SPACE STATION BUS REGULATION WITH NASA GLENN RESEARCH CENTER FLYWHEEL ENERGY STORAGE SYSTEM DEVELOPMENT UNIT

Peter E. Kascak
Ohio Aerospace Institute
Brook Park, Ohio 44142

Barbara H. Kenny
National Aeronautics and Space Administration
Glenn Research Center
Cleveland, Ohio 44135

Timothy P. Dever
QSS Group, Inc.
Brook Park, Ohio 44142

Walter Santiago
National Aeronautics and Space Administration
Glenn Research Center
Cleveland, Ohio 44135

Ralph H. Jansen
Ohio Aerospace Institute
Brook Park, Ohio 44142

ABSTRACT

An experimental flywheel energy storage system is described. This system is being used to develop a flywheel based replacement for the batteries on the International Space Station (ISS). Motor control algorithms which allow the flywheel to interface with a simplified model of the ISS power bus, and function similarly to the existing ISS battery system, are described. Results of controller experimental verification on a 300 W· hr flywheel are presented. Keywords: flywheel, motor control, battery, charge, discharge, charge reduction.

INTRODUCTION

A developmental flywheel test facility has been built at NASA Glenn Research Center (GRC), in Cleveland, Ohio. This system includes a carbon composite high-speed flywheel, which is coupled to a motor/generator, and is suspended by active magnetic bearings. This test facility allows development and testing of control algorithms for the flywheel motor/generator and magnetic bearings. Flywheel based energy storage systems are being considered as a possible replacement for the battery based system currently in use on the ISS because flywheel systems feature longer life, higher efficiency and greater depth of discharge than battery based systems. In order to allow direct replacement, the flywheel system must be made to operate in the same fashion as the battery systems currently in place on the ISS. This paper describes motor/generator control algorithms which allow the flywheel system to interface with a simplified version of the ISS electrical bus, enabling the flywheel to be "charged" by storing energy mechanically in the wheel, and "discharged" by converting mechanical energy to current on the bus, while regulating bus voltage.

NOMENCLATURE

I^*_{charge} – charge current setpoint
I^*_{DC} – DC current regulator setpoint
i^r_{ds} – d-axis current in the rotor reference frame
i^r_{qs} – q-axis current in the rotor reference frame
I^*_{CRD} – current set point for charge reduction/discharge modes
$I_{flywheel}$ – DC Current into the Flywheel
I_{load} – load current
$I_{s/a}$ – solar array current
ISS – International Space Station
BCDU/BS – Battery Charge Discharge Unit/Battery System
L_{ds} – d-axis stator inductance, H
p – time derivative operator (d/dt)
P – number of poles
$P_{flywheel}$ – Power on the AC side of the inverter
R_S – Stator resistance per phase, Ω
SAS – Solar Array System
SAW – Solar Array Wings
SSU – Sequential Shunt Unit
V_{dc} – DC bus Voltage
v^r_{ds} – d-axis voltage in the rotor reference frame
v^r_{qs} – q-axis voltage in the rotor reference frame
$V^*_{s/a}$ – Sequential Shunt Unit voltage set point
$V^*_{discharge}$ – flywheel (or BCDU) discharge voltage set point
λ_{af} – flux due to the rotor magnets

ISS POWER BUS CONFIGURATION

Power for the ISS is generated by the station solar array system (SAS), which includes the solar array wings (SAW) and the sequential shunt unit (SSU). Since the SAS cannot generate energy within the 35 minute eclipse period of the 92 minute ISS Earth orbit, some energy needs to be stored aboard the ISS. Presently, this energy is stored and regulated in a battery-based system called a Battery Charge Discharge Unit/Battery System (BCDU/BS). In order for a flywheel system to replace the BCDU/BS on the ISS, it must mimic the electrical performance of the BCDU/BS. In the following text, present BCDU/BS operation is described, and required flywheel operation is notated in parentheses. Figure 1 is a schematic of the present BCDU/BS (proposed flywheel) system.

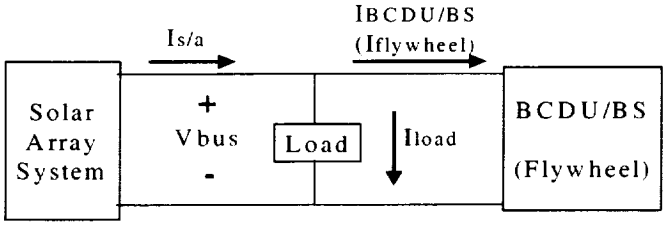

Figure 1: Block Diagram of ISS BCDU/BS (Flywheel) Power System

The BCDU/BS (flywheel) has three operational modes - the "charge" mode, the "discharge" mode, and the "charge reduction" mode. These modes of operation are summarized in Table 1.

Mode	BCDU/BS (Flywheel) DC Current	Regulated Bus Voltage
Charge	$I_{BCDU/BS} = I^*_{charge}$ ($I_{Flywheel} = I^*_{charge}$)	$V_{bus} = V^*_{s/a}$
Discharge	$I_{BCDU/BS} < 0$ ($I_{Flywheel} < 0$)	$V_{bus} = V^*_{discharge}$
Charge Reduction	$I^*_{charge} > I_{BCDU/BS} > 0$ ($I^*_{charge} > I_{Flywheel} > 0$)	$V_{bus} = V^*_{discharge}$

Table 1: BCDU/BS (Flywheel) Modes of Operation

Charge mode on the energy storage system occurs when the SAS is generating enough current to supply the ISS user (designated by the "load" in Figure 1), and to charge the batteries (accelerate the flywheel) at its charge mode current setpoint. In this mode, ISS DC bus regulation is provided by the SAS. This charge mode typically takes place when the station is in full sun.

Discharge mode on the energy storage system occurs when the batteries are discharging (flywheel is decelerating) and providing power to the load. In this mode, the BCDU (flywheel) regulates the DC bus voltage at $V^*_{discharge}$. This discharge mode typically takes place when the station is in full eclipse.

Charge reduction mode on the energy storage system occurs when the SAS provides some current, but not enough to both supply the load and charge the batteries (accelerate the flywheel) at the charge mode current setpoint. In this mode, the BCDU (flywheel) provides regulation of the DC bus at $V^*_{discharge}$. This charge reduction mode typically takes place when the station is in partial sun.

FLYWHEEL TEST CONFIGURATION

A simplified schematic of the flywheel test configuration is presented in Figure 2. In this system, the ISS bus is modeled using a commercially available DC power supply as the source, and a resistor as the load. For charge mode operations, the supply was set to 60V and 30A current limit; for discharge mode, the current limit of the supply was brought down to 0A. The load resistance value was changed to simulate different loading conditions during discharge mode. Although the flywheel is rated at 60,000 RPM, speed was limited to under 10,000 RPM during controller testing. The input filter to the inverter was a 13.2 mF capacitor.

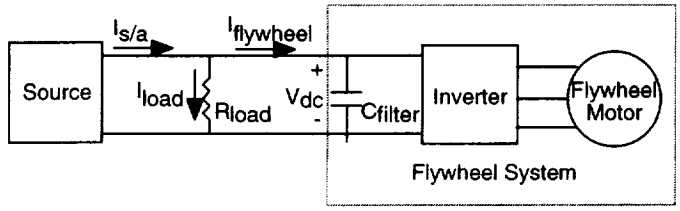

Figure 2: Simplified Flywheel Test Configuration

The entire motor/generator portion of the flywheel development system is shown schematically in Figure 3; this system includes the hardware presented in Figure 2, along with details of the motor control system and the DC bus controls. A commercially available computer was used for the controller (DC bus control system design and operation is described in detail in the following sections). The motor control signals are converted via a PWM board, and passed on to a commercially available inverter, which drives the flywheel motor. Inverter power was supplied by the simplified ISS bus (see Figure 2). Feedback signals for the controller include two motor phase currents (I_a and I_b), the motor once around (OAR) signal, and the DC bus current and voltage (I_{dc} and V_{dc}).

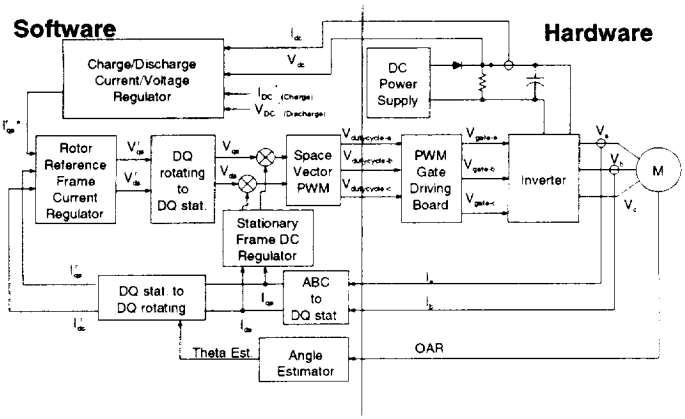

Figure 3: Flywheel System Control Software/Hardware Configuration

DC BUS CONTROL OVERVIEW

The DC bus controller must control the flywheel motor such that the dc bus current, $I_{flywheel}$, (in charge mode) and the dc bus voltage, V_{dc}, (in discharge mode) are regulated. This is done in the block labeled "Charge/Discharge Current/Voltage Regulator" (CDCVR) in Figure 3. The input variables to this block are the commanded and measured values of the dc bus voltage and current. The output variable is the current command to the inner loop motor control algorithm (i^r_{qs}). This motor control algorithm is based on the field orientation technique that is described in [1].

The CDCVR block for the DC bus control consists of three main functions:

1. Regulate the dc charge current to the flywheel system, $I_{flywheel}$, to the commanded value, I^*_{charge}, set by a higher-level ISS control during charge mode.
2. Regulate the station DC bus voltage, V_{dc}, to commanded value, $V^*_{discharge}$, set by the higher-level ISS control during charge reduction and discharge modes.
3. Transition smoothly between charge, charge reduction and discharge modes.

Two types of CDCVR controls were investigated: proportional-integral (PI) control, and PI plus feedforward control.

CDCVR PROPORTIONAL INTEGRAL (PI) CONTROL

The PI version of the CDCVR control configuration is shown in Figure 4. This PI control configuration consists of two control loops, the DC voltage loop (for discharge mode and charge reduction mode) and the DC current loop (for charge mode), and also two transition conditions.

When the flywheel system is in charge mode, the $I^*_{flywheel}$ switch is in position 1 making it equal to I^*_{charge}. At this stage, the output of the PI regulator sets the inner loop motor current command, i^{r*}_{qs}, based on the error between the commanded flywheel current (I^*_{charge}) and the measured flywheel current ($I_{flywheel}$, as defined in Figure 2). In the charge mode, $I_{flywheel}$ is positive and the solar array system (SAS) regulates the dc bus voltage.

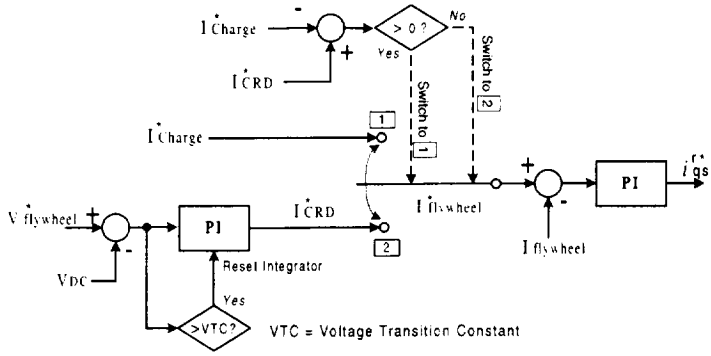

Figure 4: PI CDCVR Control Algorithm

When the flywheel system is in discharge mode or charge reduction mode, the $I^*_{flywheel}$ switch is in position 2 (see Figure 4) making it equal to I^*_{CRD}. In these modes, the flywheel system regulates the dc bus voltage by using the two PI loops connected in series. The first PI loop, going from left to right on Figure 4, processes the voltage error between the commanded dc bus voltage, $V^*_{flywheel}$ and the measured dc bus voltage, V_{dc}. The output of this 1st PI loop generates I^*_{CRD}, which is the charge reduction and discharge mode current set point that feeds the 2nd PI loop. In discharge mode, the flywheel system is providing power to the station loads thus $I_{flywheel}$ as defined in Figure 2 is negative. In charge reduction mode, the flywheel is charging, and thus $I_{flywheel}$ is positive. In either case, the flywheel system provides the dc bus voltage regulation.

From the perspective of the flywheel control system, there is really only one transition point. The flywheel control system is either set to regulate the flywheel current (charge mode) or the dc bus voltage (charge reduction and discharge modes).

In current regulation (charge mode), the solar array provides enough current to supply all of the load demand plus the charge current set point, I^*_{charge}. As the solar array moves into eclipse, the current that the array can provide drops off. The dc bus voltage will begin to fall because the solar array can't provide enough current to meet both the load demand and the charge current set point to the flywheel system. Once the dc bus voltage falls below a certain level, the flywheel system must transition from current regulation to voltage regulation and begin to regulate the dc bus voltage.

In voltage regulation (charge reduction and discharge modes) the flywheel system is regulating the dc bus. As the solar array moves out of eclipse, it can provide more and more

current. Once $I_{flywheel}$ reaches the charge current set point, I^*_{charge}, it is an indication that the solar array is now producing enough current to provide all of the station loads plus I^*_{charge}. At this point, the flywheel system must transition from voltage regulation to current regulation and the solar array system will begin to regulate the dc bus voltage.

Current and voltage regulation are detected in the PI CDCVR Control in the following way and will be described using an example. Starting in charge mode, the dc bus voltage, V_{dc}, is at 130 volts, controlled by the solar array. The flywheel voltage set point, $V^*_{flywheel}$, is at 120 volts. The voltage transition constant (VTC) is –5 volts (see Figure 4). Thus in charge mode, $V^*_{flywheel}$- V_{dc} is less than the VTC (-10 < -5) and the integrator is not reset. These conditions produce a I^*_{CRD} value larger than I^*_{charge}, which causes the $I^*_{flywheel}$ switch to move to position 1 (charge mode).

As the solar arrays move into eclipse, the dc bus voltage falls. As the bus voltage falls below 125 volts, $V^*_{flywheel}$- V_{dc} falls below the VTC, and the integrator resets to 0. This sets I^*_{CRD} to a small positive number. Since I^*_{CRD} is now less than I^*_{charge}, the $I^*_{flywheel}$ switch is moved to position 2 and the system transitions into voltage regulation (charge reduction/discharge mode).

As long as the flywheel current, $I_{flywheel}$, is less than the charge set point current, I^*_{charge}, the system remains in voltage regulation because the solar arrays are not providing enough current to meet the load demands and the current charge set point. As the station moves out of eclipse, the SAS begins to contribute current, increasing the bus voltage (V_{dc}) until $V^*_{flywheel}$- V_{dc} drops below VTC. At this point, voltage PI loop integrator will no longer be reset, I^*_{CRD} will exceed I^*_{charge}, and the $I^*_{flywheel}$ switch will move to position 1, transitioning the system to current regulation (charge mode).

CDCVR PI PLUS FEEDFORWARD CONTROL

The PI control described in the previous section and in Figure 4 is structured such that the inner loop motor command current, i^{r*}_{qs}, is derived from a PI controller operating on a $I^*_{flywheel}$ command. In charge mode, $I^*_{flywheel}$ is equal to the charge current set point, I^*_{charge}. In discharge mode, $I^*_{flywheel}$ is equal to I^*_{CRD}, the charge reduction/discharge current set point. In either case, i^{r*}_{qs} is the output of a PI control operating on the error between $I^*_{flywheel}$ and $I_{flywheel}$.

There is another approach to producing the motor current command based on the desired $I_{flywheel}$ value that is shown in Figure 5. In this approach, the open loop steady state relationship between i^r_{qs} and $I_{flywheel}$ is used to determine i^{r*}_{qs} from $I^*_{flywheel}$. This approach allows the use of a feedforward command for both voltage and current regulation, which results in a fast response with lower gains on the PIs. The lower PI gains result in less noise in the system as will be shown in the experimental results section.

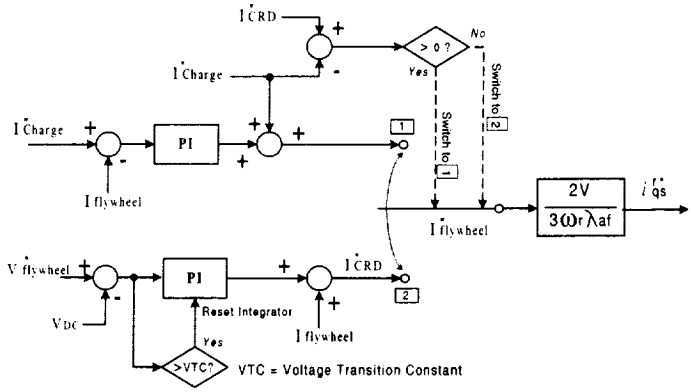

Figure 5: PI Plus Feedforward CDCVR Control Algorithm

The relationship between i^r_{qs} and $I_{flywheel}$ is based on the steady state power balance between the dc power going into the inverter and the ac power going into the flywheel motor. The ac power used by the flywheel motor can be expressed as shown in (2)[3].

$$P_{flywheel} = \frac{3}{2}(v^r_{qs}i^r_{qs} + v^r_{ds}i^r_{ds}) \qquad (2)$$

Neglecting minor losses in the inverter, the dc power supplied will equal the ac power used by the flywheel motor.

$$V_{DC}I_{DC} = \frac{3}{2}(v^r_{qs}i^r_{qs} + v^r_{ds}i^r_{ds}) \qquad (3)$$

In the motor control algorithm used in this system, i^r_{ds} is regulated to 0 [1]. Therefore the power balance in (3) is reduced to

$$V_{DC}I_{DC} = \frac{3}{2}(v^r_{qs}i^r_{qs}) \qquad (4)$$

The q-axis voltage equation is [2]

$$v^r_{qs} = i^r_{qs}R_S + L_{qs}pi^r_{qs} + i^r_{ds}\omega_r L_{ds} + \omega_r\lambda_{af} \qquad (5)$$

In steady state, the derivative term is zero. Furthermore the d-axis current is regulated to zero. Therefore (5) reduces to

$$v^r_{qs} = i^r_{qs}R_s + \omega_r\lambda_{af} \qquad (6)$$

Substituting (6) into (4), the power balance equation results in the following relation

$$V_{DC}I_{DC} = \frac{3}{2}((i^r_{qs}R_s + \omega_r\lambda_{af})i^r_{qs}) \qquad (7)$$

R_S is small compared to the back emf term, $\omega_r\lambda_{af}$, especially at high speeds, so the power balance can be approximated as

$$V_{DC} I_{DC} \cong \frac{3}{2}(\omega_r \lambda_{af} i_{qs}^r) \qquad (8)$$

This can be used to relate a current command on the dc side of the inverter to a current command on the ac side of the inverter:

$$i_{qs}^r = \frac{2V_{DC} I_{DC}^*}{3\omega_r \lambda_{af}} \qquad (9)$$

From (9) it can be seen that during current regulation (charge mode) the feedforward command to the motor current is

$$i_{qs}^{r*} = \frac{2V_{DC} I_{charge}^*}{3\omega_r \lambda_{af}} \qquad (10)$$

Figure 5 shows that the charge current set point, I_{charge}^*, sums with the output of the PI regulator that operates on the error between I_{charge}^* and $I_{flywheel}$. Under current regulation (charge mode), $I_{flywheel}^*$ is equal to this sum. If the feedforward relationship of (10) is exactly accurate, then the contribution of the PI portion to $I_{flywheel}^*$ will be zero. However, approximations were made in the derivation of (10) plus the back emf constant, λ_{af}, may not be known exactly. So the PI is used to make up for any errors in the feedforward calculation. However, the feedforward portion is contributing most of the $I_{flywheel}^*$ command so the gains on the PI can be set lower than in the previous case (PI only algorithm).

Similarly for voltage regulation (discharge and charge reduction modes) the feedforward command to the motor current is

$$i_{qs}^{r*} = \frac{2V_{flywheel}^* I_{flywheel}}{3\omega_r \lambda_{af}} \qquad (11)$$

Figure 5 also shows that $I_{flywheel}$ sums with the output of the PI regulator that process the error between $V_{flywheel}^*$ and V_{dc}. Under voltage regulation (discharge and charge reduction modes), $I_{flywheel}^*$ is equal to this sum. Similar to the current regulation (charge mode) control loop, the feedforward portion of the voltage regulation loop is contributing most of the $I_{flywheel}^*$ command so the PI gains can be set to lower values.

Furthermore, Figure 5 shows the $I_{flywheel}^*$ command converted to the i_{qs}^{r*} command through the power balance relationship of (9). For current regulation, V in this block is equal to the measured value V_{dc}. For voltage regulation, V in this block is equal to the commanded value, $V_{flywheel}^*$. In both cases, the speed, ω_r, is measured and used as an input to this block.

The transition characteristics between current regulation and voltage regulation for this PI plus feedforward control are the same as described in the previous section for the PI only control.

EXPERIMENTAL RESULTS

To verify the proper operation of the two described control loops and prove that the flywheel system can perform like a BCDU/BS, two types of tests were performed. The first test was a step change on the charge set point and the second test was a load step while the flywheel was in discharge mode. These tests were performed on both the PI and the PI plus feedforward controllers.

The two controllers were tuned to have similar responses. This was achieved by using approximately 1 order of magnitude higher gains for the PI only control than the PI plus feedforward control. There was very little difference between the PI only and the PI with feedforward performance in the response of the DC bus variables, $I_{flywheel}$ and V_{dc}. Thus for the DC bus variables, only the results for the PI plus feedforward control are presented.

Figure 6 shows the response to a step change in commanded current during charge mode. The transient response time was about 12 msec. As mentioned previously, the combination of the SAW and SSU is experimentally modeled using a DC power supply. Because the measurement of DC current is taken on the power supply side of the capacitor, most of the current transient is caused by the reaction of the power supply to the change in current taken by the flywheel system.

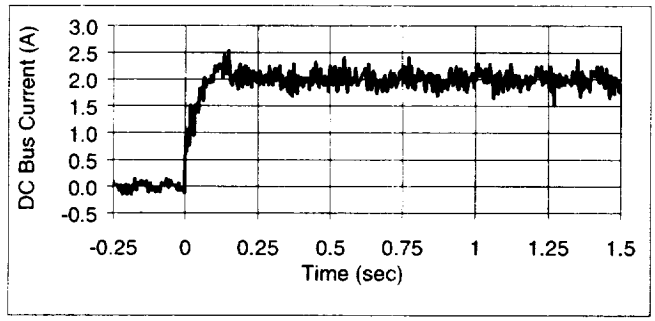

Figure 6: $I_{flywheel}$ Response for Charge Mode Current Step Change Using PI Plus Feedforward Control Algorithm

Figure 7 shows the system operating in discharge mode (flywheel system regulating the dc bus voltage) with a step change in load. Discharge mode is experimentally modeled with the power supply turned off, therefore the step response is entirely due to the flywheel system. The discharge voltage set point, $V_{flywheel}^*$, is set to 60 volts. Figure 7 clearly shows that the bus voltage regulation is maintained for this load step.

Figure 8 shows the flywheel speed for the same load step shown in Figure 7. It can be seen that when the load is applied the slope of the speed trace becomes more negative. This is because more power is taken from the flywheel system and delivered to the load.

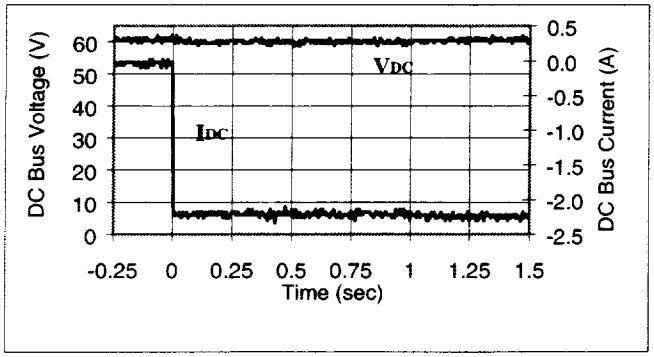

Figure 7: Discharge Mode Load Step Change – Voltage and Current Response (PI Plus Feedforward Control Algorithm)

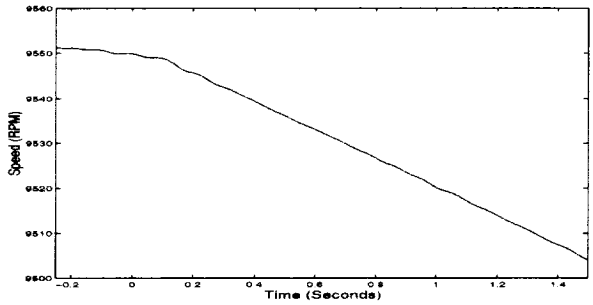

Figure 8: Discharge Mode Load Step Change – Speed Response (PI Plus Feedforward Control Algorithm)

Figures 9 and 10 show the flywheel system motor phase current response for the same load step shown in Figure 7 for pure PI and PI plus feed foward controllers respectively. It is clear that the phase currents for the pure PI controller are much noisier than with the PI plus feedforward controller. This is because the correcting PI loop on the PI plus feedforward controller can have very small gains due to the action of the feedforward portion of the control. The pure PI controller requires larger gains to achieve similar performance; these large gains increase the control bandwidth, allowing the controller to act on noisy feedback signals (i.e. the DC bus voltage).

CONCLUSIONS

DC bus regulation during changes in charge current set point and discharge load value was demonstrated on the flywheel development unit. Additionally, CDCVR regulator mode transition algorithms were implemented and discussed. These results demonstrate that a flywheel system can successfully mimic the operating modes of the ISS battery system. This is an important milestone because it is a first step in demonstrating the feasibility of replacing the ISS battery system with a flywheel system.

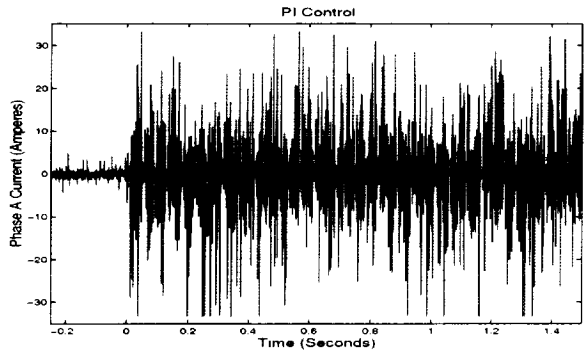

Figure 9: Discharge Mode Load Step Change – Phase Current Response (PI Control Algorithm

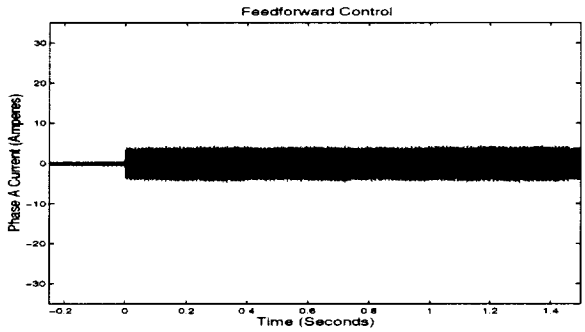

Figure 10: Discharge Mode Load Step Change – Phase Current Response (PI Plus Feedforward Control Algorithm)

CDCVR regulators using PI and PI plus feedforward compensation were implemented and tested, and the results were presented. Although the pure PI controller is simpler, the resulting motor phase currents are noisier. This phase current noise is irrelevant to the DC bus control; however, it does cause energy loss and unnecessary heating of the flywheel motor.

REFERENCES

[1] Kenny, B., P. Kascak, H. Hofmann, M. Mackin, W. Santiago, R. Jansen, "Advanced Motor Control Test Facility For NASA GRC Flywheel Energy Storage System Technology Development Unit," *to be published at 2001 IECEC*, Savannah, Georgia.

[2] Krishnan, Ramu, *Permanent Magnet Synchronous and Brushless DC Motor Drives: Theory, Operation, Performance, Modeling, Simulation, Analysis and Design*, Virginia Tech., Blacksburg, Virginia, 1999.

[3] Novotny, D.W. and T.A. Lipo, "*Vector Control and Dynamics of AC Drives*," Oxford Science Publications, Oxford, 1996.

REPORT DOCUMENTATION PAGE

Form Approved
OMB No. 0704-0188

1. AGENCY USE ONLY (*Leave blank*)	2. REPORT DATE	3. REPORT TYPE AND DATES COVERED
	September 2001	Technical Memorandum

4. TITLE AND SUBTITLE

International Space Station Bus Regulation With NASA Glenn Research Center Flywheel Energy Storage System Development Unit

5. FUNDING NUMBERS

WU-755-1A-09-00

6. AUTHOR(S)

Peter E. Kascak, Barbara H. Kenny, Timothy P. Dever, Walter Santiago, and Ralph H. Jansen

7. PERFORMING ORGANIZATION NAME(S) AND ADDRESS(ES)

National Aeronautics and Space Administration
John H. Glenn Research Center at Lewis Field
Cleveland, Ohio 44135-3191

8. PERFORMING ORGANIZATION REPORT NUMBER

E-12993

9. SPONSORING/MONITORING AGENCY NAME(S) AND ADDRESS(ES)

National Aeronautics and Space Administration
Washington, DC 20546-0001

10. SPONSORING/MONITORING AGENCY REPORT NUMBER

NASA TM—2001-211138
IECEC2001-AT-10

11. SUPPLEMENTARY NOTES

Prepared for the 36th Intersociety Energy Conversion Engineering Conference cosponsored by the ASME, IEEE, AIChE, ANS, SAE, and AIAA, Savannah, Georgia, July 29–August 2, 2001. Peter E. Kascak and Ralph H. Jansen, Ohio Aerospace Institute, 22800 Cedar Point Road, Brook Park, Ohio 44142; Barbara H. Kenny and Walter Santiago, NASA Glenn Research Center; Timothy P. Dever, QSS Group, Inc., 2001 Aerospace Parkway, Brook Park, Ohio 44142. Responsible person, Barbara H. Kenny, organization code 5450, 216–433–6289.

12a. DISTRIBUTION/AVAILABILITY STATEMENT

Unclassified - Unlimited
Subject Categories: 20 and 33 Distribution: Nonstandard

Available electronically at http://gltrs.grc.nasa.gov/GLTRS
This publication is available from the NASA Center for AeroSpace Information, 301–621–0390.

12b. DISTRIBUTION CODE

13. ABSTRACT (*Maximum 200 words*)

An experimental flywheel energy storage system is described. This system is being used to develop a flywheel based replacement for the batteries on the International Space Station (ISS). Motor control algorithms which allow the flywheel to interface with a simplified model of the ISS power bus, and function similarly to the existing ISS battery system, are described. Results of controller experimental verification on a 300 W·hr flywheel are presented.

14. SUBJECT TERMS

Flywheel energy storage; Permanent magnet synchronous machine; Motor drives; Field orientation control; Flywheel; Motor control; Battery; Charge; Discharge; Charge reduction

15. NUMBER OF PAGES

12

16. PRICE CODE

17. SECURITY CLASSIFICATION OF REPORT	18. SECURITY CLASSIFICATION OF THIS PAGE	19. SECURITY CLASSIFICATION OF ABSTRACT	20. LIMITATION OF ABSTRACT
Unclassified	Unclassified	Unclassified	